ACS APPLIED MATERIALS & INTERFACES

Research Article

www.acsami.org

Organo-Chlorinated Thin Films Deposited by Atmospheric Pressure Plasma-Enhanced Chemical Vapor Deposition for Adhesion Enhancement between Rubber and Zinc-Plated Steel Monofilaments

Cédric Vandenabeele,[†,‡,∥] Simon Bulou,*[,†] Rémy Maurau,[†,⊥] Frederic Siffer,[§] Thierry Belmonte,[‡] and Patrick Choquet[†]

[†]Luxembourg Institute of Science and Technology, 41 rue du Brill, Belvaux, L-4422, Luxembourg

[‡]Institut Jean Lamour, UMR 7198 CNRS, Département de Chimie et Physique des Solides et des Surfaces, Université de Lorraine, Parc de Saurupt, CS 50840, Nancy F-54011, France

[§]The Goodyear Tire & Rubber Company, Avenue Gordon Smith, Colmar-Berg, L-7750, Luxembourg

Supporting Information

ABSTRACT: A continuous-flow plasma process working at atmospheric pressure is developed to enhance the adhesion between a rubber compound and a zinc-plated steel monofilament, with the long-term objective to find a potential alternative to the electrolytic brass plating process, which is currently used in tire industry. For this purpose, a highly efficient tubular dielectric barrier discharge reactor is built to allow the continuous treatment of "endless" cylindrical substrates. The best treatment conditions found regarding adhesion are Ar/O_2 plasma pretreatment, followed by the deposition from dichloromethane of a 75 nm-thick organo-chlorinated plasma polymerized thin film. Ar/O_2 pretreatment allows the removal of organic residues, coming from drawing lubricants, and induces external growth of zinc oxide. The plasma layer has to be preferably deposited at low power to conserve sufficient hydrocarbon moieties. Surface analyses reveal the complex chemical mechanism behind the establishment of strong adhesion levels, more than five times higher after the plasma treatment. During the vulcanization step, superficial ZnO reacts with the chlorinated species of the thin film and is converted into porous and granular bump-shaped $Zn_wO_xH_yCl_z$ nanostructures. Together, rubber additives diffuse through the plasma layer and lead to the formation of zinc sulfide on the substrate surface. Hence, two distinct interfaces, rubber/thin film and thin film/substrate, are established. On the basis of these observations, hypotheses explaining the high bonding strength results are formulated.

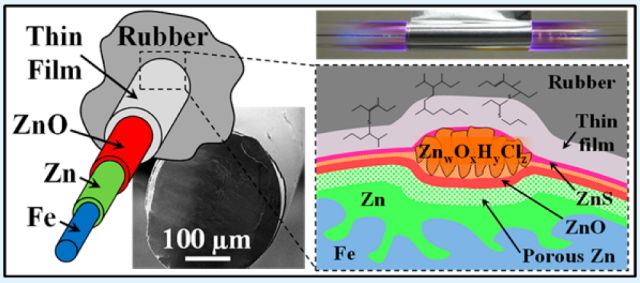

KEYWORDS: *plasma-enhanced chemical vapor deposition, continuous-flow deposition process, atmospheric pressure, organo-chlorinated thin films, surface preparation, interface characterization, rubber−steel adhesion*

1. INTRODUCTION

Since the development of radial tire in 1946, steel cords are become the principal strengthening elements in specific regions of a tire, such as the belt, carcass, and bead.[1,2] To ensure performance and durability of the final product throughout its service life, a strong adhesion is required between the rubber and its reinforcing materials. As steel itself has very poor adhesion to rubber, steel wires are usually electrolytically coated with brass before entering the tire manufacturing line. Indeed, bonds formed between rubber and brass are very strong and resistant to dynamic loading.

The mechanism behind this bonding is first introduced by Van Ooij in the late 1970s,[3,4] but further details and modifications to the formulated mechanism are brought since then.[1,2,5−9] It is known that the rubber/brass interface forms during the rubber vulcanization step. At an early stage of curing, zinc ions and copper ions move to the surface of brass by cationic diffusion and react with sulfurating species contained in the rubber. This reaction leads to the formation of sulfide layers, with predominantly nonstoichiometric copper sulfide Cu_xS and smaller amounts of zinc sulfide ZnS.

After many years of study, it is still not fully understood how the sulfide layers interact with the rubber, but it is thought that high bond strength is obtained primarily by a mechanical anchorage between the rubber and a 50 nm-thick Cu_xS layer. Indeed, the copper sulfide grows as dendrites into the viscous rubber, which is still viscoelastic at this stage of curing. When the sulfide growth levels off, cross-linking occurs and the result is a strong interlocking of the cured rubber and the Cu_xS layer. The strength of this mixed rubber/Cu_xS interface is further enhanced

Received: April 2, 2015
Accepted: June 12, 2015
Published: June 12, 2015

DOI: 10.1021/acsami.5b02887
ACS Appl. Mater. Interfaces 2015, 7, 14317−14327

by van der Waals forces generated between the rubber and the large surface area of the copper sulfide layer.[10] It is also generally accepted that covalent bonds are formed between copper, sulfur, and carbon (Cu−S−C−...),[11,12] but their contribution to rubber/brass adhesion is considered as minor. Another important aspect that emerges from the revised model proposed by Van Ooij[5] is that the concentration of cross-linking species (i.e., species inducing cross-linking) is much higher in the immediate vicinity of the interface than in the bulk of the compound. Then, the network adjacent to the brass is denser, which increases subsequently the adhesion force.

Although the brass plating process is very efficient, it suffers from several disadvantages. The first one is the high cost of the process. Indeed, the brass electrodeposition process requires important energy consumption for the thermal annealing post-treatment.[13] The rising cost of copper is also prejudicial. Moreover, electrodeposition of brass implies the use of great quantities of chemicals and is not a renewable treatment.

But the most discussed weakness of this process is the rubber/brass interface degradation over time, mainly in conditions of high temperature and humidity that are often encountered during the service life of a tire.[1,2,4] This degradation is even more damaging for truck tires that are generally retreaded (i.e., only tread is replaced when worn, the tire armature being conserved). Toxic and expensive cobalt salts are then added to the rubber formulation to increase the interface lifetime.[1,2,4,14−16]

Regarding these limitations, there is an interest in developing a cheaper process with reduced environmental impact to promote adhesion between rubber and steel. Attempts are made to replace the brass coating by another metallic coating like a bilayer Zn/Ni on Zn/Co system[17−20] or a simple Zn/Co monolayer.[13,20,21] It turns out that adhesion as strong as the one with brass can be obtained, with sometimes a much better resistance to aging and with potential reduction costs for the synthesis of the metallic coating. With these configurations, the origin of adhesion is generally attributed to a ZnS bonding layer, whose structure is modified by the presence of cobalt to become compatible with the establishment of a strong bonding. This demonstrates that ZnS structure can be, in some circumstances, in adequacy with adhesion build-up. Unfortunately, cobalt salts are still essential in the compound formulation for the rubber/metal bond formation and consequently, these new processes cannot overcome the inherent drawbacks of the cobalt element.

The use of plasma polymer thin films deposited on the steel surface is also explored, plasma processes being solvent-free and, therefore, environmentally cleaner processes.[22−30] The major advantage of plasma polymerization for metal treatment holds in the possibility to deposit very thin (<100 nm) and highly cross-linked uniform films. These films have low solubility and high thermal stability. Furthermore, the ability to clean the substrate and to deposit a thin film in a single reactor provides a great deal of process control and versatility in a large-scale industrial production line for coating continuously metallic substrates.[23]

Different precursors are tested to produce the adhesive layer, such as acetylene,[23−29] butadiene,[29] or thiophene.[30] In all these studies, thin film deposition is carried out in reactors working at low pressure. Substrates used are steel sheets, except for the studies carried out by Kang et al.,[29] where thin films are deposited on zinc-plated steel filaments. One of the major prerequisite that stands out from these studies is the necessity to deposit an optimized thickness of thin film to reach the highest adhesion levels, which are comparable, in the best cases, to those obtained with brass. Another prerequisite is the need to preserve acetylenic or olefinic groups in the thin layer to ensure cross-linking between the rubber and the plasma polymerized film. Except for the case of thiophene, a two-interface system is generally observed. Understanding adhesion thus requires considering both the metal/thin film interface and the thin film/rubber interface. However, only few data are available about the implied mechanisms.

In this work, we aim at studying the adhesive interlayer made by an organo-chlorinated plasma polymerized thin film, deposited from dichloromethane on "endless" zinc-plated steel filaments, by using a continuous-flow plasma deposition process working at atmospheric pressure. The interest and the feasibility of such a treatment are described in a previous paper.[31] The main conclusions drawn from this previous work are that, by carefully setting the plasma parameters, defect-free coatings, homogeneous in thickness and composition, can be deposited in a dynamic mode on several meters of metallic filament, with dynamical deposition rates ranging from 0.4 to 1.2 nm m s^{-1}. The hydrogen content in the layer is shown to decrease when the power injected into the discharge increases, leading to a more and more inorganic thin film, resembling more carbon black or even graphite than hydrocarbons. Various volatile chlorinated species (e.g., HCl, Cl_2, ...) are produced in the discharge during the deposition process and some of them are trapped in the coating. These species could have an impact on health and environment that will have to be considered for a large scale industrial development. Nevertheless, the aim of this work is to present the new interface produced owing to the innovative process developed, and to bring in a fundamental scientific approach, elements to understand the complex underlying mechanisms. Thus, these health and environmental concerns are not discussed in this paper and will be discussed in a future work. In our previous works,[31] only thin film deposition is studied. For the adhesion issue that is presented herein, the surface preparation has also to be considered. Then, we begin by describing the conditions of surface preparation and thin film deposition that give the best adhesion levels between the rubber and the plasma-coated, zinc-plated steel filament. Next, we investigate the new interface formed in this configuration and propose a mechanism to explain the excellent adhesion obtained with the plasma polymer coating.

2. EXPERIMENTAL SECTION

The substrate used is a 300 μm in diameter zinc-plated steel monofilament, supplied by Bekaert (Kortrijk, Belgium). The zinc thickness is heterogeneous because of the underlying steel roughness. It is generally lower than 200 nm, but it can exceed locally one micrometer where zinc penetrates in notches present on steel surface during drawing (Figure 1). Brass-plated steel monofilaments from the same supplier and with the same diameter are also used as reference.

The precursor employed to produce the organo-chlorinated thin film is analytic grade dichloromethane, from Merck (purity >99.8%). Discharge gases are argon and oxygen (Air Liquide, 99.999%). The rubber is an experimental proprietary compound from Goodyear. It contains, inter alia, polyisoprene, carbon black, sulfur, zinc oxide, stearic acid, antioxidants, and cyclohexyl benzothiazole sulfenamide (CBS) accelerator. No cobalt salt is present in the rubber, one of the objectives being to get rid of this element.

The reactor used is a homemade tubular dielectric barrier discharge (DBD), which is described in details and sketched elsewhere.[31] A rolling system moves the substrate through the quartz tube (34 cm long for pretreatment, 15 cm long for thin film deposition) where the discharge is generated. The high voltage electrode is an aluminum electrode (10 cm long for pretreatment, 2.5 cm long for thin film deposition) placed

DOI: 10.1021/acsami.5b02887
ACS Appl. Mater. Interfaces 2015, 7, 14317−14327

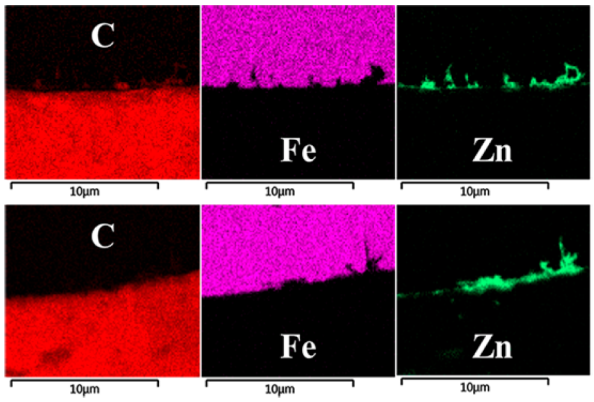

Figure 1. Cross-sectional EDX (energy dispersive X-ray) mapping of the zinc-plated steel monofilament embedded in an epoxy resin. Two samples are presented, top and bottom.

around the quartz tube. The grounded electrode is the wire itself, supported by a grounded metallic pulley.

The precursor injection system, the high voltage source, and gas flow controllers are also described in a previous paper.[31] For the whole study, the precursor flow is set at 0.16 standard cubic centimeters per minute (sccm), equivalent to 2.5 mmol min^{-1}, the gas flow (Ar or Ar + O_2) is fixed at 10 standard liters per minute (slm), and the high voltage frequency is set at 20 kHz. The power delivered to the discharge is always the incident power, that is, the power directly read on the generator. The real power dissipated in the discharge is measured by the *Lissajous method* depending on the incident power, and can also be found in ref 31.

Adhesion between the rubber and the zinc-plated steel monofilament is measured by using the Standard Bead wire Adhesion Test (SBAT), which is an ASTM (American Society for Testing and Materials) procedure. It consists of measuring the force that has to be applied for extracting the monofilament from the vulcanized rubber block in which it has been embedded. Vulcanization is realized in a stainless steel mold, which allows introducing seven monofilaments simultaneously in the rubber, and which is placed in a JBT Engineering heating press. Vulcanization conditions are 428 K (155 °C), 2×10^7 Pa (200 bar), 15 min. Embedment length (i.e., the length of monofilament that is embedded in rubber) is 12.7 mm. Adhesion tests are realized at least 8 h after vulcanization, by using a Tinius Olsen H1KT instrument that pulls the monofilaments with a traction speed of 50 mm min^{-1}.

The desired thin film thickness is deposited by adjusting the linear speed of the monofilament through the DBD-reactor, based on previous dynamical deposition rate measurements.[31] For instance, at 10 W, the measured dynamical deposition rate is 0.42 nm m s^{-1}. Therefore, the linear speed has to be adjusted at 0.56 cm s^{-1} to obtain a 75 nm-thick thin film. In these conditions, the time required to coat 1 m of monofilament is about 3 min. The indicated residence time in the discharge corresponds to the time necessary for a point of the monofilament to cover the electrode length. It is thus underestimated as the discharge expands from both electrode extremities.

Scanning electron microscopy (SEM) and energy dispersive X-ray (EDX) analyses are performed with a Hitachi SU70 HRSEM. Atomic force microscopy analyses (AFM) are done on a Molecular Imaging PICO SPM LE.

X-ray photoelectron spectroscopy (XPS) analyses are realized on a Kratos Axis-Ultra DLD device, with an X-ray beam (monochromatic Al Kα line (1486.6 eV)) irradiating a 1×2 mm^2 area. 110×110 μm^2 areas, in the center of the irradiating area, are selected, through iris and diaphragm present in the X-ray column, and analyzed. Pass energy is fixed at 40 eV. In these conditions, the curvature of the analyzed substrates can produce an error on the quantification, related to the fact that our samples are composed of different layers and that the photoelectrons do not come from the same depth depending on the position of the analyzed area. This error is considered as minor (difference in depth analysis lower than 7% on the whole analyzed area) and thus, does not affect the interpretation of the data.

Secondary ion mass spectrometry (SIMS) depth profiles are performed on a CAMECA SC-Ultra device. Sample sputtering is done with a Cs^+ ion beam (1 keV, 2 nA) that scans a 200×200 μm^2 area. Detected secondary ions MCs^+ (where M is O, Fe, and Zn) come from a 60 μm in diameter circular area, located in the center of the Cs^+-irradiated area.

Time-of-flight secondary ion mass spectrometry (TOFSIMS) analyses are done on an ION-TOF TOF.SIMS.[5] Static analyses are performed with a pulsed Bi_3^+ beam (25 kV, 0.4 pA), used to irradiate a 150×150 μm^2 area (PIDD = 5.12×10^{11} ions/cm^2). Mappings are realized in "burst" mode. The calibration is done on C^+, CH^+, CH_2^+, CH_3^+, $C_2H_3^+$, and $C_2H_5^+$ ions in positive mode, and on CF^-, CH^-, CH_2^-, C_2H^-, and C_4H^- ions in negative mode. For TOFSIMS profiling, sample sputtering is performed with a Cs^+ ion beam (10 kV, 16.5 nA) that creates a 100×100 μm^2 crater; 20×20 μm^2 areas, in the center of the sputtered region, are analyzed with a pulsed Bi_3^+ beam (25 kV, 0.4 pA). These 20×20 μm^2 areas are supposed to be flat enough to be sputtered everywhere with the same rate. The difference in height between the highest positions (center of the analyzed zone) and the lowest positions (edges of the analyzed zone), because of the curvature of the sample, is about 320 nm. This distance (320 nm), compared with the distance covered by secondary ions in the TOFSIMS analyzer (~2 m from the sample to the detector), corresponds to an error $\Delta M/M = 320 \times 10^{-9}/2 = 1.6 \times 10^{-7}$. Thus, the error in mass between 2 identical ions coming from the center or the edges of the analyzed area is about 0.2 ppm. Because the resolution of the TOFSIMS used is 50 ppm, the error induced by the sample curvature on secondary ions identification is negligible.

For TOFSIMS profiles, a sacrificial aluminum layer is first deposited prior to starting the analyses, with a sputtering deposition equipment from Kurt J. Lesker Company. The interest of this sacrificial layer is to let sufficient time to negative ions X^- to form Cs_2X^+ clusters with Cs^+ ions used for sample sputtering, during the first steps of profiling. The filter paper used is "Hardened Ashless" circle filter from Whatman, type 540.

Focused ion beam (FIB) milling and transmission electron microscopy (TEM) analyses are done at Case Western Reserve University (Cleveland, OH, USA), respectively on a FEI Helios Nanolab 650 device and a Zeiss Libra 200EF device.

3. RESULTS AND DISCUSSION

3.1. Investigations of Optimal Treatment Conditions for Adhesion. We investigate the best treatment conditions for enhancing adhesion between the rubber and the zinc-plated steel monofilament, coated with the plasma polymerized organo-chlorinated thin film. Through the different experiments done, it appears that both the substrate surface preparation and the plasma layer have to be optimized to get high adhesion levels.

To determine the best surface preparation, adhesion strengths are measured between the rubber and the substrate coated with the same plasma thin film, but previously prepared by different surface cleaning processes. The plasma layer is 75 nm-thick, deposited with an injected power of 10 W (these conditions are justified later). The different surface processes tested are solvent cleaning, performed by rubbing the steel filament with laboratory wipes soaked in acetone first and ethanol next, and plasma cleaning. The plasma cleaning is realized either in argon or in an argon/oxygen mixture.

Ar cleaning is studied by varying both the injected power and the residence time in the discharge in the ranges 20−100 W and 4−60 s, respectively, without any significant effect on adhesion levels. Cleaning in an Ar/O_2 mixture is more sensitive. A too "harsh" Ar/O_2 pretreatment (i.e., a high duration pretreatment with a high injected power) leads to a weakening of the steel filament, resulting in a strong drop of its tensile strength. This weakening is attributed to the heat treatment brought by the

DOI: 10.1021/acsami.5b02887
ACS Appl. Mater. Interfaces 2015, 7, 14317−14327

plasma that affects the structure of the steel and reduces the mechanical properties of the filament. Therefore, the study ranges for Ar/O_2 cleaning have to be limited, either by limiting the power for a long residence time, or by limiting the residence time for a high power. Two couples of conditions that do not lead to a substrate weakening are determined: (40 W, 60 s) and (80 W, 4 s). Measured adhesion strengths are similar for these two couples of conditions. Oxygen content in the discharge is also studied, without noticeable influence on the substrate tensile strength or adhesion values in the range 0.5−10%.

Adhesion strength measurements are depicted in Figure 2. Adhesion levels are also measured directly after substrate

Figure 2. Adhesion level measurements between the rubber and the zinc-plated steel monofilament, coated with a 75 nm-thick organo-chlorinated plasma thin film. Surfaces are previously cleaned by different ways (the red line is the highest tensile strength of the filament).

preparation (solvent or plasma cleaning) to be sure that adhesion enhancement comes from the plasma layer and not only from the pretreatment. The indicated values represent the mean value over five measurements. Experimental conditions are (80 W, 4 s) for Ar cleaning, and (80 W, 4 s, 0.5% O_2) for Ar/O_2 cleaning.

Surface preparation is a critical stage to obtain high adhesion levels. The use of an Ar/O_2 plasma appears to be the best solution for pretreatment as it leads to adhesion levels stronger than the tensile strength of the steel filament, that is, higher than 230 N. These results are comparable to those obtained in the case of brass-plated steel monofilaments. In these conditions, the adhesion strength is multiplied by a factor of 5, compared with the initial adhesion level (i.e., adhesion between rubber and untreated zinc-plated steel filament). It can be noted that the same Ar/O_2 pretreatment without plasma coating gives the lowest adhesion level obtained in this study. Indeed, adhesion strength falls down to 20 N, compared with the 45 N obtained for the zinc-plated monofilament reference.

Extensive studies are performed to determine the effect of Ar/O_2 pretreatment on the substrate surface (see Supporting Information). It emerges from these studies that plasma cleanings are more efficient than chemical cleaning with solvents as surface preparation, in that they remove drawing lubricant residues "in-depth", namely, in furrows dug in the substrate by the drawing dies, and that unlike plasma cleaning with argon, Ar/O_2 pretreatment involves the external growth of ZnO on the substrate surface, which becomes rougher. In extreme conditions of Ar/O_2 pretreatment, the metallic zinc layer can even be completely converted into ZnO.

This above-mentioned Ar/O_2 pretreatment is the best preparation whatever the thin film properties. Therefore, the parameters of this pretreatment are selected for the optimization of the plasma coating described hereinafter.

To determine the thin film properties that give the strongest bonding, adhesion levels are measured after coating the substrate with plasma layers of different thicknesses, deposited with different injected powers: 10, 30, and 50 W. Adhesion measurements with the rubber are reported in Figure 3.

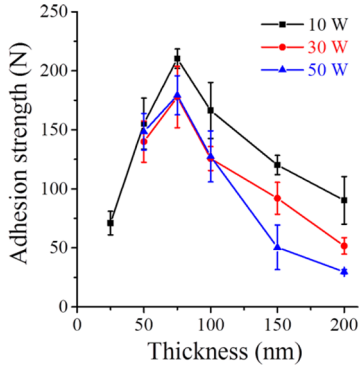

Figure 3. Adhesion level measurements between the rubber and the zinc-plated steel monofilament pretreated by Ar/O_2 plasma and coated with an organo-chlorinated plasma thin film. Influence of thin film thickness and injected power during deposition.

One can observe that whatever the power, maximum adhesion levels are obtained for a 75 nm-thick plasma layer. The existence of a critical thickness can be interpreted either by the need to regulate the chemical reactions that occur during the adhesion interface formation (by bringing the right quantity of reactants), or by the necessity to regulate the diffusion rates of species from the substrate or from the rubber through the plasma layer. We can add that a too thick film can lead to a weak boundary layer, which is not suitable for an adhesion issue.

Moreover, for a fixed thickness, an increase in the injected power leads to a decrease in adhesion strengths. Based on our previous works,[31] in which we show that increasing the power leads to a reduction of hydrocarbons content in the thin film that becomes more and more inorganic, it seems that the plasma layer has to keep some chemical groups, for example, unsaturated hydrocarbons, to allow cross-linking between the organo-chlorinated coating and the rubber.

As a conclusion for the optimization study, obtaining of a strong adhesion interface between the rubber and the zinc-plated steel monofilament requires to carefully clean the substrate surface and to deposit a thin film with well-defined properties. The best pretreatment is performed in an Ar/O_2 plasma that removes organic residues and oxidizes the surface, thus increasing the thickness of the native ZnO layer on the substrate surface. This ZnO thickening is detrimental to adhesion if the zinc-plated steel monofilament is directly embedded in the rubber after surface preparation. Indeed, it is well-known that ZnO formation passivates the substrate surface and prevents reaction with the rubber.[1,2,4,5] In contrast, if the Ar/O_2 prepared monofilament is coated with the organo-chlorinated layer, the ZnO coverage becomes beneficial for adhesion. This observation suggests that superficial ZnO is converted during vulcanization, under the action of the plasma layer species, into a structure that is advantageous, or even requisite, for the building of the adhesion interface. Concerning plasma deposition, the optimal

DOI: 10.1021/acsami.5b02887
ACS Appl. Mater. Interfaces 2015, 7, 14317−14327

thickness is 75 nm. The coating has to be preferably deposited at low power, probably to conserve unsaturated hydrocarbons in the layer, and to make cross-linking with the rubber possible.

3.2. Formation of Adhesion Interface. To observe the effects of the plasma layer on the substrate surface during vulcanization, SEM and TOFSIMS analyses are performed on the monofilament surface treated in the optimized conditions. A first sample is analyzed directly after thin film deposition. A second one is analyzed after annealing in an oven heated at 428 K (155 °C) to reproduce the temperature conditions encountered during vulcanization, and during 30 min, that is, two times longer than the curing process, to accentuate the occurring phenomena and make them more easily observable. Related SEM pictures are given in Figure 4.

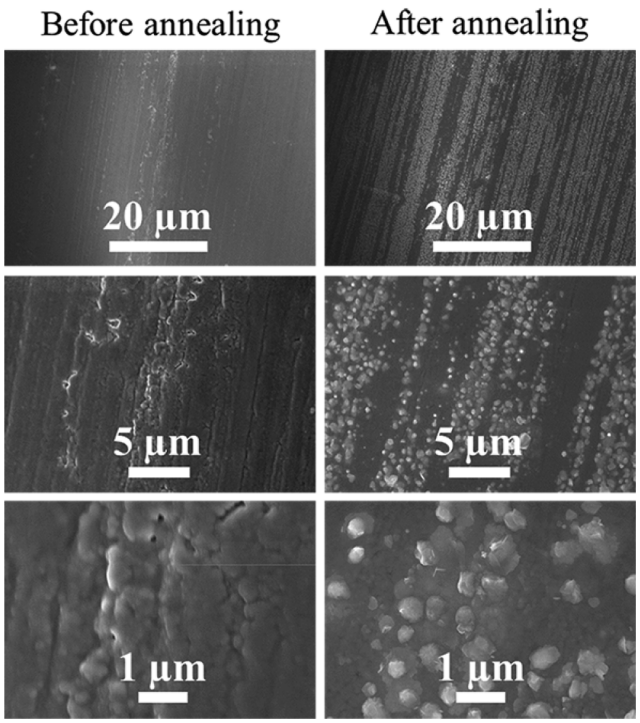

Figure 4. SEM observations of the zinc-plated steel monofilament surface, pretreated by Ar/O_2 plasma and coated with a 75 nm-thick organo-chlorinated thin film deposited at 10 W. (Left) Directly after thin film deposition. (Right) After introducing the coated monofilament in a 428 K heated oven during 30 min.

A significant difference can be observed between the two samples, that is, emergence of series of bumps, about 500 nm in diameter, on the annealed sample. These bumps cover the whole surface, they are aligned along the monofilament axis direction and they follow the drawing lines. It is thus likely that bumps formation is accelerated in these regions because of the presence of cracks, which are associated with a higher surface energy or with stimulated diffusion rates. At a larger scale, one can observe on the nonannealed sample (bottom-left picture) that a sketch of these bumps begins to emerge on the surface. This may indicate that bumps formation is strongly accelerated by the rise in temperature.

Carbon and chlorine maps performed by TOFSIMS on the annealed sample surface (Figure 5) show that these bumps appear in bright on the chlorine map and in dark on the carbon map. Therefore, these bumps are made of carbon-free inorganic chlorinated species.

TOFSIMS mass spectra recorded from the surface of both samples are depicted in Figure 6. A periodical repetition of the same sequences of peaks is visible on the mass spectrum related to the sample after annealing. By comparing these sequences with reference isotopic distributions, it is possible to undoubtedly assign them to $(ZnO)_xZn^+$, $(ZnO)_xZnOH^+$, and $(ZnO)_xZnCl^+$ crystals. As a consequence, the inorganic chlorinated species composing the bumps can be designated as $Zn_wO_xH_yCl_z$. Among these species, one can find zinc oxide ZnO, zinc hydroxide $Zn(OH)_2$, zinc chloride $ZnCl_2$, zinc hydroxychloride Zn(OH)Cl, or more complex structures, such as simonkolleite $Zn_5(OH)_8Cl_2$.

The thermal annealing induces structural changes in the thin film that make possible the emergence of these bumps from the plasma layer and their observation by TOFSIMS, whose depth analysis is about 1 nm. However, to determine if such structural changes occur in the real situation, that is, when the coating is caught between the rubber and the substrate, the adhesion interface formed between the rubber and the coated monofilament after vulcanization is directly observed by TEM (Figure 7) after a FIB milling preparation.

On these TEM pictures, the plasma layer can be quite clearly distinguished between the rubber and the substrate, which indicates the establishment of two distinct interfaces: rubber/thin film and thin film/substrate. The plasma coating is uniform in thickness and follows the substrate morphology. Indeed, the thin film goes above the bumps and lies over them. Bumps are not homogeneous and exhibit a porous and granular structure (Figure 7B and C). A further magnification is necessary to more clearly observe the metallic zinc layer (Figure 7D). Voids are visible inside the bump and it is thus possible that the thin film penetrates into these pores to get a mechanical anchoring enhancing adhesion.

To investigate now the diffusion mechanisms that occur during vulcanization, TOFSIMS depth profiles are performed across the adhesion interface, by using the filter paper preparation method.[9,10] It consists of placing a filter paper between rubber and the coated steel filament during vulcanization. This filter paper prevents the transport of the largest species (rubber polymers or carbon black), while more volatile species responsible for sulfidation, like sulfur or accelerators, can diffuse through it. Thus, physicochemical processes occur normally, but no bonding between rubber and metal can be generated. Thereby, it is possible to delaminate rubber and metal and to obtain rubber-free sample surfaces for analysis.

To better understand the role of the plasma coating, this analysis is also realized on a monofilament embedded in the rubber directly after Ar/O_2 plasma cleaning. No plasma polymer thin film is deposited in this case and a very weak adhesion level is observed. TOFSIMS profiles of positive ions are depicted in Figure 8. For the sake of clarity, each spectrum is normalized to its maximum intensity.

Sample sputtering being done with highly energetic Cs^+ beam, only atomic or diatomic information are obtained. Negative ions are detected under the form Cs_2X^+, while positive ions are detected under the form CsY^+.

On both profiles, the first signal detected is $CsAl^+$, which corresponds to the sacrificial aluminum layer. Then, while the $CsZn^+$ signal, corresponding to the electrodeposited zinc layer, grows rapidly in the case of the sample embedded in rubber directly after Ar/O_2 cleaning (Figure 8A), a signal of Cs_2Cl^+, which can be assigned to the organo-chlorinated thin film, starts first growing in the case of the coated sample (Figure 8B). The Cs_2Cl^+ signal is not complete due to the saturation of the

DOI: 10.1021/acsami.5b02887
ACS Appl. Mater. Interfaces 2015, 7, 14317−14327

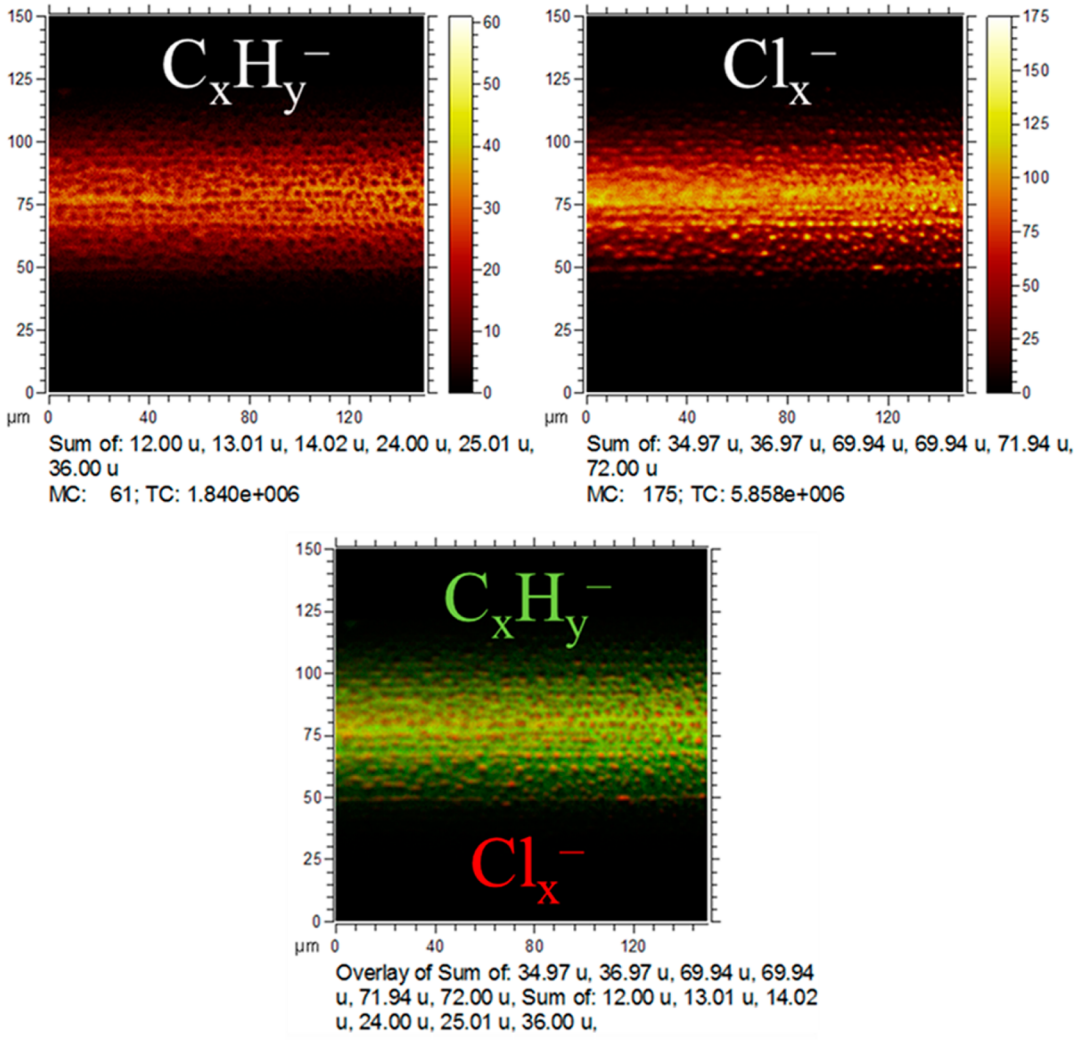

Figure 5. TOFSIMS maps performed on the zinc-plated steel monofilament surface, pretreated by Ar/O_2 plasma and coated with a 75 nm-thick organo-chlorinated thin film, after annealing in an oven (428 K for 30 min).

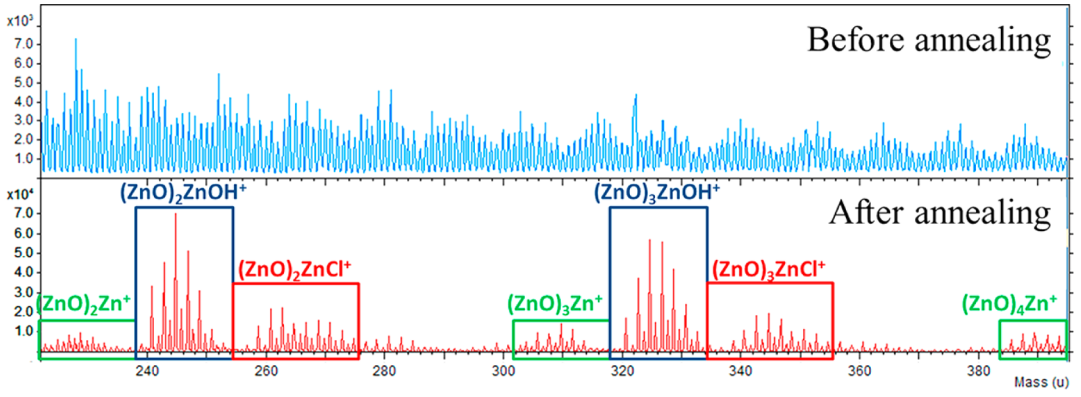

Figure 6. TOFSIMS mass spectra recorded from the zinc-plated steel monofilament surface, pretreated by Ar/O_2 plasma and coated with a 75 nm-thick organo-chlorinated thin film. (Top) Directly after thin film deposition. (Bottom) After annealing in an oven (428 K for 30 min).

detectors. The maximum intensity of $CsZn^+$ signal is preceded by the maxima of Cs_2ZnO^+, Cs_2O^+, Cs_2ZnS^+, Cs_2S^+, and Cs_2CN^+ signals, with additionally $CsZnCl^+$ signal in the case of the coated sample (Figure 8B), representative of the $Zn_wO_xH_yCl_z$ layer.

In the case of the uncoated sample (Figure 8A), Cs_2ZnO^+ and Cs_2O^+ signals correspond to the ZnO layer, while Cs_2ZnS^+ and Cs_2S^+ signals indicate the formation of a zinc sulfide layer on the substrate surface, which does not allow here the creation of a bond with the rubber. The Cs_2CN^+ signal can be interpreted either by the presence of residual contamination or by rubber species adsorbed on the monofilament surface. It is also true for Cs_2S^+ signal.

In the case of the coated-sample (Figure 8B), the detection of the Cs_2ZnO^+ signal between $CsZn^+$ and $CsZnCl^+$ signals

DOI: 10.1021/acsami.5b02887
ACS Appl. Mater. Interfaces 2015, 7, 14317−14327

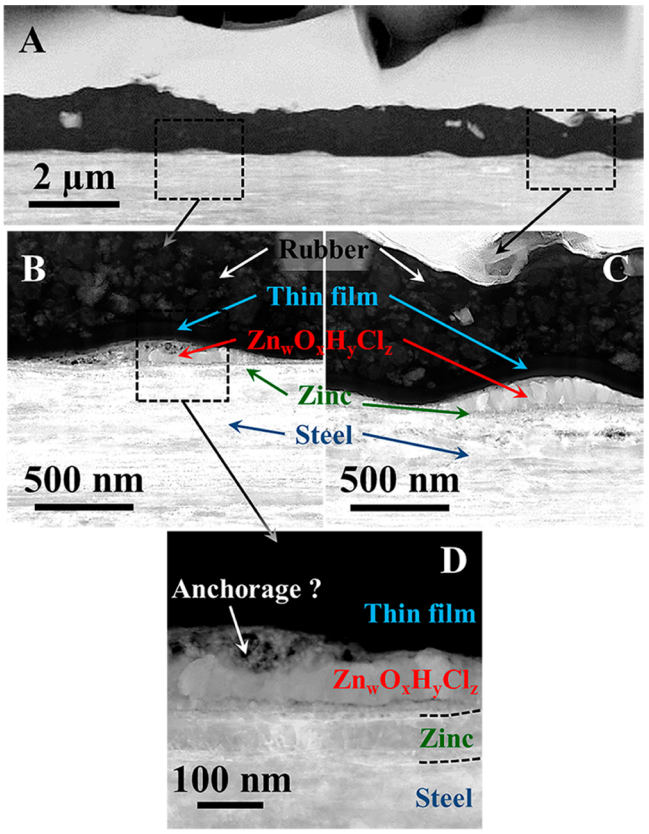

Figure 7. (A–D) TEM pictures of the adhesion interface established between the rubber and the zinc-plated steel monofilament, pretreated by Ar/O_2 plasma, and coated with a 75 nm-thick organo-chlorinated thin film. Black dotted lines are added to distinguish the electro-deposited zinc (D).

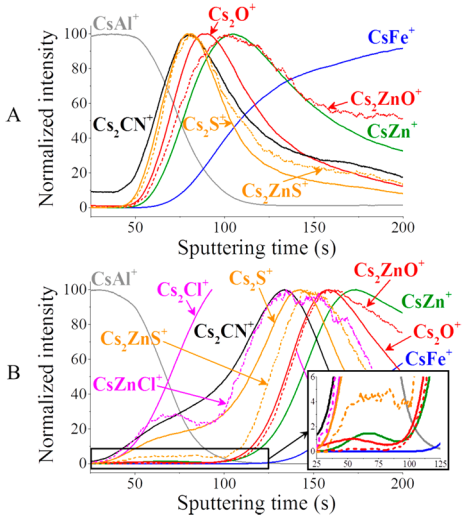

Figure 8. Normalized TOFSIMS depth profiles performed on zinc-plated steel monofilaments embedded in rubber by using the filter paper method. Sacrificial aluminum layers are deposited before to start profiling. (A) Monofilament embedded in rubber after Ar/O_2 plasma cleaning, associated with a low adhesion level (~20 N). (B) Monofilament embedded in rubber after Ar/O_2 plasma cleaning and 75 nm-thick thin film deposition, associated with a high adhesion value (>230 N).

indicates that the conversion of ZnO into $Zn_wO_xH_yCl_z$ is not total. Moreover, the detection of Cs_2ZnS^+, Cs_2S^+, and Cs_2CN^+ signals indicates that rubber species are able to diffuse across the plasma layer to form ZnS on the substrate surface.

The main difference between the two profiles is the presence of a shouldering of several species for sputtering times between 25 and 100 s, in the case of the coated sample. This shouldering is consistent with the bump-shaped morphology of the $Zn_wO_xH_yCl_z$ layer, as schematized in Figure 9.

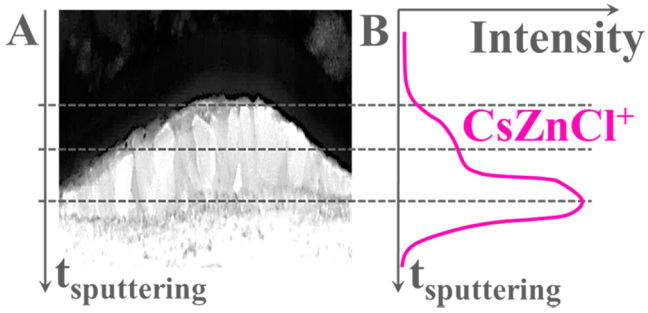

Figure 9. Interpretation of the shape of the $CsZnCl^+$ signal in the TOFSIMS mass spectrum related to the coated sample. (A) TEM picture of a $Zn_wO_xH_yCl_z$ bump, in cross view (the picture is distorted to make the figure clearer). (B) Associated $CsZnCl^+$ signal.

The fact that this shouldering is also present on the Cs_2ZnS^+ signal indicates that the formation of zinc sulfide follows the surface morphology induced by the conversion of ZnO.

SEM pictures of the coated monofilament surface recovered after vulcanization with the filter paper can be seen in Figure 10.

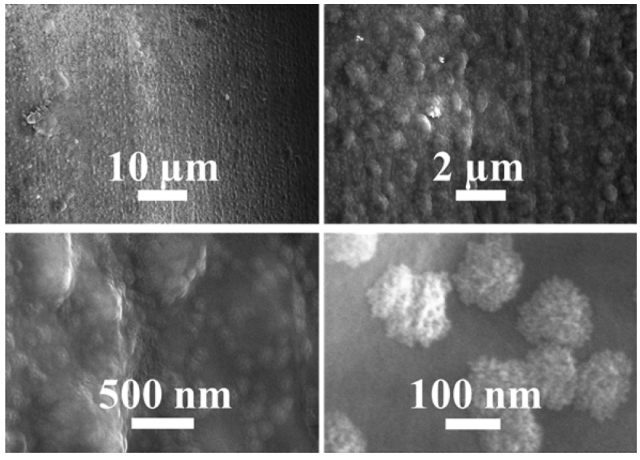

Figure 10. SEM pictures of the coated monofilament surface after vulcanization with the filter paper.

Similarities can be observed with the coated monofilament introduced in the oven (Figure 4), such as $Zn_wO_xH_yCl_z$ bumps, but this time, structural changes in the film that make emerge the bumps from the plasma layer have not occurred. Indeed, bumps are still covered with the organo-chlorinated thin film. Here, we see the thin film/rubber interface, which cannot have been transformed into an adhesion interface due to the presence of the filter paper. In addition to $Zn_wO_xH_yCl_z$ bumps, smaller structures, about 100 nm in diameter, are also visible. At this scale, no chemical analysis can have been performed to identify these structures. Nevertheless, according to TEM pictures of the adhesion interface (Figure 7), where brighter structures are observed in the rubber, these smaller structures could

DOI: 10.1021/acsami.5b02887
ACS Appl. Mater. Interfaces 2015, 7, 14317–14327

correspond to rubber species trapped in the topmost part of the film, or also to the first growth steps of $Zn_wO_xH_yCl_z$ bumps.

3.3. State of Knowledge and Adhesion Origin. According to the different analyses and characterizations done, a growth mechanism is now proposed to explain the origin of adhesion.

The initial state of the substrate surface is schematized in Figure 11A. The steel monofilament is protected from corrosion

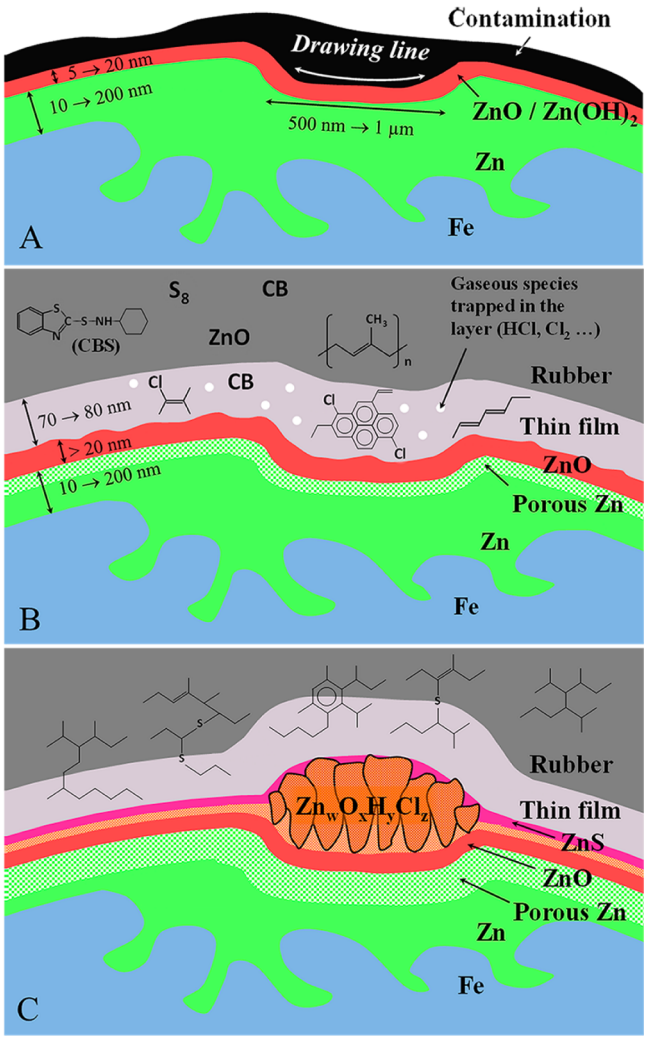

Figure 11. Cross-sectional sketch of (A) initial substrate surface, (B) substrate surface pretreated by Ar/O_2 plasma, coated with organo-chlorinated plasma thin film, and contacted with the rubber, just before vulcanization, and (C) adhesion interface formed after vulcanization. Sketches are not to scale.

by an electrodeposited metallic zinc layer. Exposure to the atmosphere during the cooling step after drawing leads to the formation of native zinc oxide and hydroxide layers on the metallic zinc surface (Figure S2, Supporting Information). Besides, organic contaminations, coming from the used liquid drawing lubricants, cover the substrate surface in an inhomogeneous way and encrust in surface furrows dug by drawing dies (Figures S1 and S2, Supporting Information).

Surface contamination is removed during Ar/O_2 plasma pretreatment, during which organic residues react physically or chemically with energetic and reactive species of the plasma. The main phenomenon is likely the oxidation of the contamination, which produces volatile oxidative products that are evacuated by the gas flow.[32,33] The substrate overheating during this pretreatment also induces a thickening of the ZnO layer (Figure S3, Supporting Information), whose surface becomes rougher, as evidenced by AFM analyses (Figure S4, Supporting Information). An outward surface oxidation probably occurs, governed by the diffusion of zinc ions from the metallic zinc layer toward the surface and their reaction with oxygen ions or reactive oxygen-containing species from the plasma. Although it has not been demonstrated, the diffusion of zinc ions is likely accompanied by the inward diffusion of cation vacancies from ZnO to Zn metal, provoking the so-called Kirkendall effect where the metallic zinc layer becomes porous at the Zn/ZnO interface.

After this substrate pretreatment step, an organo-chlorinated plasma thin film from dichloromethane, whose optimal thickness is 75 nm (Figure 3), is deposited. It has been shown in ref 31 that this film is mainly composed of carbon black (or graphite) and hydrocarbons more or less chlorinated and unsaturated, with also the presence in the layer of polycyclic aromatic hydrocarbons. It has been also evidenced that various volatile chlorinated species, like HCl and Cl_2, are trapped in the plasma layer.

After plasma deposition, the coated monofilament is put in contact with the rubber that contains all the ingredients necessary for vulcanization. The resulting system, illustrated Figure 11B, is then placed under the heating press for vulcanization.

During vulcanization, the rise in temperature stimulates diffusion mechanisms and accelerates chemical reactions. Zinc ions diffuse from the substrate toward the plasma layer. Chlorine ions, hydrogen chloride and other small chlorinated molecules diffuse from the plasma layer toward the substrate and the rubber. Sulfur-containing species in the rubber migrate across the thin film to the substrate surface.

The exact mechanism that occurs is unknown, but one of the first reactions is likely the partial conversion of ZnO into $Zn_wO_xH_yCl_z$ (Figures 6 and 8), which is induced by the attack of ZnO by chlorinated species from the plasma layer. This conversion, strongly accelerated by the rise in temperature, occurs on the whole substrate surface. Nevertheless, $Zn_wO_xH_yCl_z$ structures grow more rapidly along drawing lines, where they form porous and granular bumps, 500−1000 nm in diameter and 150−200 nm in thickness (Figures 4 and 7).

A possible chemical reaction pathway is

$$ZnO + 2HCl \rightarrow ZnCl_2 + H_2O \quad (1)$$

$$ZnCl_2 + H_2O \rightarrow Zn(OH)Cl + HCl \quad (2)$$

$$2Zn(OH)Cl + 3ZnO + 3H_2O \rightarrow Zn_5(OH)_8Cl_2 \quad (3)$$

where HCl is gaseous hydrogen chloride trapped in the thin film or formed from species of the plasma layer. Reaction 1 leads to the formation of zinc chloride and liquid water at 428 K and 2×10^7 Pa. $ZnCl_2$ being a highly hygroscopic substance, it can then absorb this water to form zinc hydroxychloride Zn(OH)Cl first and next simonkolleite $Zn_5(OH)_8Cl_2$. Too few data are available in thermodynamic tables about Zn(OH)Cl and $Zn_5(OH)_8Cl_2$ compounds to determine which species is the most stable in these given temperature and pressure conditions. Nevertheless, some studies show that simonkolleite can dehydrate when temperature rises to form first Zn(OH)Cl and then $ZnCl_2$.[34−36] Thus, it can be assumed that the opposite reaction is possible when the system cools down after vulcanization in the presence of water, with zinc chloride hydrolysis.

DOI: 10.1021/acsami.5b02887
ACS Appl. Mater. Interfaces 2015, 7, 14317−14327

Otherwise, from Figure 7, and knowing that ZnO is not totally converted, one may think that a significant volume of $Zn_wO_xH_yCl_z$ is produced from a little quantity of ZnO, and therefore, that the molar volume of the formed product is much larger than those of ZnO. This reasoning can thus be a clue of simonkolleite formation, whose molar volume is about 11 times larger than those of ZnO (see Table 1), when the system reaches equilibrium.

Table 1. Molar Volume Values of Different Zinc Derivatives, Calculated from the Molar Mass and the Volume Mass of These Derivatives, Found in the Literature

chemical species	molar mass ($g\ mol^{-1}$)	volume mass ($g\ cm^{-3}$)	molar volume ($cm^3\ mol^{-1}$)
Metallic Zn	65.41	7.13	9.17
ZnO	81.38	5.60	14.53
$Zn(OH)_2$	99.39	3.05	32.59
$ZnCl_2$	136.29	2.90	47.00
Zn(OH)Cl	117.86	?	?
$Zn_5(OH)_8Cl_2$	533.87	3.30	161.78

In parallel of ZnO conversion, sulfur-containing species diffuse across the thin film and are adsorbed on the substrate surface (Figure 8), probably on metallic zinc having diffused to the surface, or released during the conversion of ZnO (one O for one Zn) into $Zn_5(OH)_8Cl_2$ (five Zn for eight O). The result is the formation of zinc sulfide that follows the surface morphology. Uncertainty remains concerning the respective positions of the ZnS and $Zn_wO_xH_yCl_z$ layers, because $CsZnCl^+$ ions are detected before Cs_2ZnS^+ ions in TOFSIMS depth profile (Figure 8B). This behavior can be explained by considering that the ZnS/$Zn_wO_xH_yCl_z$ interface is rough due to the granular structure of $Zn_wO_xH_yCl_z$ (Figure 7C).

The state of the final system is schematized in Figure 11C. Concerning the origin of adhesion, TEM pictures of Figure 7 clearly show the establishment of two distinct interfaces substrate/thin film and thin film/rubber. Therefore, the two interfaces have to be considered to fully explain the phenomenon.

It can be noticed that the plasma layer exhibits similarities with the rubber, like the presence of unsaturated hydrocarbons and carbon black. Consequently, the plasma layer is probably able, as rubber, to cross-link by sulfur action: this element diffuses from the rubber to the substrate through the film. The plasma layer and the rubber would form thereby a common cross-linked network. Indeed, in this region, the most likely is a chemical adhesion.

The origin of adhesion in the thin film/substrate interface region seems to be related to the morphology modification. Figure 7 shows that the $Zn_wO_xH_yCl_z$ layer has a porous structure in which the thin film can penetrate and make a mechanical anchorage. Whereas these observations are not sufficiently explicit to fully attribute the adhesion to this phenomenon, the nanostructuration induced by the plasma treatment is clearly involved in the high adhesion increase.

Indeed, the bump-shaped morphology of the $Zn_wO_xH_yCl_z$ layer strongly increases the surface area between this structure and the plasma layer. This probably plays an important role in adhesion mechanisms. The increase in surface area can promote a higher density of mechanical interlocking, chemical bonds and also van der Waals interactions at the thin film/substrate interface region.

Zinc sulfide formation is also found out in this region. Some studies fully assign the rubber/steel adhesion enhancement to the presence of a bonding ZnS layer,[13,17−21] even if this layer is generally said not bonding in related reviews.[1,2,5,6] Indeed, according to Van Ooij,[5] zinc sulfide does not bond to rubber because its growth is too slow and does not form dendrites as copper sulfide does, making impossible a mechanical anchorage. However, other studies show that the presence of chlorine in the interface region can accelerate diffusion rates and lead to a thicker ZnS layer.[37,38] In our study, ZnS is also detected at the rubber/substrate interface when the zinc-plated steel filament is embedded in rubber directly after Ar/O_2 plasma pretreatment, without plasma coating (Figure 8A), and no solid bond is formed (as shown in Figure 2 by the related low adhesion strength value). Moreover, except the shouldering in the Cs_2ZnS^+ signal (Figure 8B), the ZnS layer does not seem thicker in the presence of the chlorinated layer. Therefore, if the ZnS layer plays a role in adhesion mechanisms in our situation, it is predominately due to a particular structure or geometry, coming from the fact that ZnS grows on a porous and bump-shaped $Zn_wO_xH_yCl_z$ layer.

It is also pointed out that ZnO conversion could imply the formation of zinc salts intermediate species, as for example zinc chloride $ZnCl_2$. According to certain studies,[39,40] these zinc salts can act as catalyzers for chlorinated polymers cross-linking. $ZnCl_2$ could therefore, locally, assist sulfur as a cross-linking promoter, inside the plasma layer and in the region close to the plasma layer. This would result in a higher cross-link density in the interface region, which would stabilize the bonds formed between the rubber and the zinc-plated steel monofilament coated with the organo-chlorinated thin film.

4. CONCLUSION

The adhesion mechanisms between rubber and a zinc-plated steel monofilament coated with an organo-chlorinated thin film are investigated. The thin film is deposited from dichloromethane in a continuous-flow process by using a tubular DBD reactor working at atmospheric pressure.

In the first section, we investigate the treatment conditions that improve the adhesion levels. The optimal conditions are a combination of Ar/O_2 plasma pretreatment, followed by the deposition of a 75 nm-thick plasma layer. The Ar/O_2 pretreatment removes organic contamination and leads to an external growth of zinc oxide. This plasma pretreatment has to be carefully adjusted to avoid excessive oxidation and weakening of the monofilament. Then, the plasma layer has to be preferably deposited at low power to keep a sufficient hydrocarbon content and ensure cross-linking inside the layer during rubber vulcanization. In these optimal treatment conditions, the adhesion strength is multiplied by five compared with the untreated zinc-plated steel filament. It exceeds the tensile strength of the monofilament, as in the case of the brass-plated steel monofilament reference.

In the second section, we study more specifically the adhesion interface and we propose mechanisms liable to explain the bonding generation. We show that the action of chlorinated species from the plasma layer on the substrate surface results in a partial conversion of the superficial ZnO layer into $Zn_wO_xH_yCl_z$ structures during vulcanization. These structures grow faster along drawing lines, where they form porous and granular bumps. The term $Zn_wO_xH_yCl_z$ may gather different species, such as metallic Zn, ZnO, $Zn(OH)_2$, $ZnCl_2$, Zn(OH)Cl, or $Zn_5(OH)_8Cl_2$. We also show that sulfur-containing species present in the rubber are able to diffuse through the plasma layer

DOI: 10.1021/acsami.5b02887
ACS Appl. Mater. Interfaces 2015, 7, 14317−14327

and to react with the substrate surface, leading to the formation of a zinc sulfide layer in this region.

After the vulcanization step, a two-interface system is obtained. At the rubber/thin film interface, the most likely is a chemical adhesion, due to cross-linking between the plasma layer and the rubber phase. At the thin film/substrate interface, the origin of adhesion probably involves both physical (interlocking between thin film and $Zn_wO_xH_yCl_z$ and/or ZnS, increase in cross-link density close to the interface, van der Waals interactions) and chemical contributions, which are enhanced by the increase in surface area induced by the bump-shaped growth of the $Zn_wO_xH_yCl_z$ layer.

As a conclusion, we set up a continuous atmospheric pressure plasma process, liable to be implemented at the industrial scale (by multiplying the number of reactors in series), which enhances the adhesion strength between a rubber compound and a zinc-plated steel filament, by nanostructuration of the zinc surface. The different interface analyses performed allow us to provide a consistent physicochemical reaction pathway occurring during rubber vulcanization. Thereby, we are able to propose possible mechanisms to explain the formation of the interface and the enhancement of adhesion.

This work is a first step that presents a new scientific approach to increase adhesion between zinc-plated steel wires and rubber, using an original atmospheric plasma deposition process. In order to constitute a suitable alternative process to the brass electrodeposition process, additional studies have now to be performed. Exploratory works dealing with aging resistance and increase in deposition rates are currently under investigation for this purpose and the results will be presented in a future article.

■ ASSOCIATED CONTENT

Supporting Information

Additional discussion and methods, XPS quantification of detected elements, SEM pictures of the zinc-plated steel monofilament surface, evolution of O 1s high resolution spectrum, SIMS depth profiles, and AFM 3D representations. The Supporting Information is available free of charge on the ACS Publications website at DOI: 10.1021/acsami.5b02887.

■ AUTHOR INFORMATION

Corresponding Author

*E-mail: simon.bulou@list.lu. Tel: +352 47 02 61 579.

Present Addresses

[‖]C.V.: Laboratoire de Chimie des Interactions Plasma Surface (ChIPS), CIRMAP, Université de Mons, 23 Place du Parc, Mons 7000, Belgium

[⊥]R.M.: Laboratoire de Physique Subatomique et de Cosmology, Université Grenoble-Alpes, CNRS/IN2P3, 53 Avenue des Martyrs, Grenoble 38026, France

Notes

The authors declare no competing financial interest.

■ ACKNOWLEDGMENTS

The authors would like to thank the Luxembourg Institute of Science and Technology (LIST) and the Goodyear Tire and Rubber Company for their financial support. These works were done within the framework of the LEA LIPES, a structure supported by the CNRS to whom we convey our deepest gratitude.

■ ABBREVIATIONS

CBS = cyclohexyl benzothiazole sulfenamide
sccm = standard cubic centimeters per minute
slm = standard liters per minute
SBAT = standard bead wire adhesion test
ASTM = American Society for Testing and Materials
DBD = dielectric barrier discharge
SEM = scanning electron microscopy
EDX = energy dispersive X-ray
AFM = atomic force microscopy
XPS = X-ray photoelectron spectroscopy
SIMS = secondary ion mass spectrometry
TOFSIMS = time-of-flight secondary ion mass spectrometry
PIDD = primary ion dose density
FIB = focused ion beam
TEM = transmission electron microscopy

■ REFERENCES

(1) Fulton, W. S. Steel Tire Cord−Rubber Adhesion, Including the Contribution of Cobalt. *Rubber Chem. Technol.* **2005**, *78*, 426−457.

(2) Van Ooij, W. J.; Harakuni, P. B.; Buytaert, G. Adhesion of Steel Tire Cord to Rubber. *Rubber Chem. Technol.* **2009**, *82*, 315−339.

(3) Van Ooij, W. J. Fundamental Aspects of Rubber Adhesion to Brass-Plated Steel Cords. *Rubber Chem. Technol.* **1979**, *52*, 605−675.

(4) Van Ooij, W. J. Mechanism and Theories of Rubber Adhesion to Steel Tire Cords—An Overview. *Rubber Chem. Technol.* **1984**, *57*, 421−456.

(5) Van Ooij, W. J. Rubber−Brass Bonding. In *Handbook of Rubber Bonding*; Crowther, B. G., Ed.; Rapra Technology Limited: Shrewsbury, Shropshire, U.K., 2001; Chapter 6, pp 163−195.

(6) Fulton, W. S.; Wilson, J. C. Review of Tyre Cord Adhesion. In *Handbook of Rubber Bonding*; Crowther, B. G., Ed.; Rapra Technology Limited: Shrewsbury, Shropshire, U.K., 2001; Chapter 7, pp 197−212.

(7) Kurbatov, G. C.; Beschenkov, V. G.; Zaporozchenko, V. I. AES and Factor Analysis Study of Cord-Oxidized Brass Layers and Rubber−to−Brass Interface Chemical Composition. *Surf. Interface Anal.* **1991**, *17*, 779−785.

(8) Hammer, G. E. A New Look at the Steel Cord−Rubber Adhesive Interphase by Chemical Depth Profiling. *J. Vac. Sci. Technol., A* **2001**, *19*, 2846−2850.

(9) Hotaka, T.; Ishikawa, Y.; Mori, K. Characterization of Adhesion Interlayer between Rubber and Brass by a Novel Method of Sample Preparation. *Rubber Chem. Technol.* **2007**, *80*, 61−82.

(10) Buytaert, G.; Coornaert, F.; Dekeyser, W. Characterization of the Steel Tire Cord−Rubber Interface. *Rubber Chem. Technol.* **2009**, *82*, 430−441.

(11) Beecher, J. F. X-ray Photoelectron Spectroscopic Studies of the Bonding of Phenyl Sulfides to Copper. *Surf. Interface Anal.* **1991**, *17*, 245−250.

(12) Persoone, P.; De Gryse, R.; De Volder, P. A New Powerful Transformation for Maximum Likelihood Common Factor Analysis. *J. Electron Spectrosc. Relat. Phenom.* **1995**, *71*, 225−232.

(13) Yan, H.; Downes, J.; Boden, P. J.; Harris, S. J. Use of Zinc Alloy Coatings on Steel Cord Reinforcement in Vehicle Tyres. *Trans. Inst. Met. Finish.* **1999**, *77*, 71−74.

(14) Fulton, W. S.; Smith, G. C.; Titchener, K. J. Interfacial Microanalysis of Rubber−Tyre−Cord Adhesion and the Influence of Cobalt. *Appl. Surf. Sci.* **2004**, *221*, 69−86.

(15) Chandra, A. K.; Biswas, A.; Mukhopadhyay, R.; Bhowmick, A. K. Effect of Anion in Cobalt Promoters on the Adhesion between Steel Cord and Rubber Compound. *J. Adhes.* **1994**, *44*, 177−196.

(16) Chandra, A. K.; Biswas, A.; Mukhopadhyay, R.; Bhowmick, A. K. SEM/EDX Studies of the Influence of a Cobalt Adhesion Promoter on the Interface between Rubber Skim Compounds and Tire Steel Cord. *J. Adhes. Sci. Technol.* **1996**, *10*, 431−460.

(17) Giridhar, J.; Van Ooij, W. J. Study of Zn−Ni and Zn−Co Alloy Coatings Electrodeposited on Steel Strips. I: Alloy Electrodeposition

DOI: 10.1021/acsami.5b02887
ACS Appl. Mater. Interfaces 2015, 7, 14317−14327

and Adhesion of Coatings to Natural Rubber Compounds. *Surf. Coat. Technol.* **1992**, *52*, 17−30.
(18) Giridhar, J.; Van Ooij, W. J. Study of Zn−Ni and Zn−Co Alloy Coatings Electrodeposited on Steel Strips. II: Corrosion, Dezincification and Sulfidation of the Alloy Coatings. *Surf. Coat. Technol.* **1992**, *53*, 35−47.
(19) Giridhar, J.; Van Ooij, W. J. Adhesion and Corrosion Properties of a New NiZn/ZnCo-Coated Steel Tire Cord. *Surf. Coat. Technol.* **1992**, *53*, 243−255.
(20) Orjela, G.; Harris, S. J.; Vincent, M.; Tommasini, F. Improved Tyre Safety and Life by a New Wire/Rubber Adhesion System. *Kautsch. Gummi Kunstst.* **1997**, *50*, 776−785.
(21) Cipparrone, M.; Pavan, F.; Orjela, G. Alternatives to Brass for Coating Tire Steel Cord. *Wire J. Int.* **1998**, *31*, 78−82.
(22) Blenner, D. R.; Boenig, H. V. Method for Bonding Elastomers to Metals. U.S. Patent 4,396,450A, August 2, 1983.
(23) Tsai, Y. M.; Boerio, F. J.; Van Ooij, W. J.; Kim, D. K.; Rau, T. Surface Characterization of Novel Plasma-Polymerized Primers for Rubber-to-Metal Bonding. *Surf. Interface Anal.* **1995**, *23*, 261−275.
(24) Tsai, Y. M.; Boerio, F. J.; Kim, D. K. Infrared Spectroscopy of Interphases between Model Rubber Compounds and Plasma Polymerized Acetylene Films. *J. Adhes.* **1995**, *55*, 151−163.
(25) Tsai, Y. M.; Boerio, F. J.; Kim, D. K. Adhesion of Natural Rubber Compounds to Plasma Polymerized Acetylene Films. *J. Adhes.* **1997**, *61*, 247−270.
(26) Tsai, Y. M.; Boerio, F. J. Molecular Structure of Interfaces Between Plasma-Polymerized Acetylene Films and Steel Substrates. *J. Appl. Polym. Sci.* **1998**, *70*, 1283−1298.
(27) Boerio, F. J.; Tsai, Y. M.; Kim, D. K. Adhesion of Natural Rubber to Steel Substrates: The Use of Plasma Polymerized Primers. *Rubber Chem. Technol.* **1999**, *72*, 199−211.
(28) Bertelsen, C. M.; Boerio, F. J.; Kim, D. K. Plasma Polymerized Primers for Rubber-to-Steel Bonding. *Wire J. Int.* **2002**, *35*, 122−125.
(29) Kang, H. M.; Chung, K. H.; Kaang, S.; Yoon, T. H. Enhanced Adhesion of Steel Filaments to Rubber via Plasma Etching and Plasma-Polymerized Coatings. *J. Adhes. Sci. Technol.* **2001**, *15*, 467−481.
(30) Delattre, J. L.; d'Agostino, R.; Fracassi, F. Plasma-Polymerized Thiophene Films for Enhanced Rubber−Steel Bonding. *Appl. Surf. Sci.* **2006**, *252*, 3912−3919.
(31) Vandenabeele, C.; Maurau, R.; Bulou, S.; Siffer, F.; Gerard, M.; Belmonte, T.; Choquet, P. Continuous Deposition of Organo-Chlorinated Thin Films by Atmospheric Pressure Dielectric Barrier Discharge in a Wire-Cylinder Configuration. *Plasma Processes Polym.* **2014**, *11*, 1089−1101.
(32) Baravian, G.; Chaleix, D.; Choquet, P.; Nauche, P. L.; Puech, V.; Rozoy, M. Oil Removal from Iron Surfaces by Atmospheric-Pressure Barrier Discharges. *Surf. Coat. Technol.* **1999**, *115*, 66−69.
(33) Thiébaut, J. M.; Belmonte, T.; Chaleix, D.; Choquet, P.; Baravian, G.; Puech, V.; Michel, H. Comparison of Surface Cleaning by Two Atmospheric Pressure Discharges. *Surf. Coat. Technol.* **2003**, *169−170*, 186−189.
(34) Srivastava, O. K.; Secco, E. A. Studies on Metal Hydroxy Compounds. I. Thermal Analyses of Zinc Derivatives ε-$Zn(OH)_2$, $Zn_5(OH)_8Cl_2{\cdot}H_2O$, β-ZnOHCl, and ZnOHF. *Can. J. Chem.* **1967**, *45*, 579−583.
(35) Garcia-Martinez, O.; Vila, E.; Martin de Vidales, J. L.; Rojas, R. M.; Petrov, K. On the Thermal Decomposition of the Zinc(II) Hydroxide Chlorides $Zn_5(OH)_8Cl_2{\cdot}H_2O$ and β-Zn(OH)Cl. *J. Mater. Sci.* **1994**, *29*, 5429−5434.
(36) Tanaka, H.; Fujioka, A. Influence of Thermal Treatment on the Structure and Adsorption Properties of Layered Zinc Hydroxychloride. *Mater. Res. Bull.* **2010**, *45*, 46−51.
(37) Jeon, G. S.; Han, M. H.; Seo, G. Effect of Tetrachlorobenzoquinone on the Adhesion between Rubber Compound and Brass-Plated Steel Cord. *J. Adhes.* **1999**, *69*, 39−57.
(38) Jeon, G. S.; Seo, G. Promotion Effect of a Chlorotriazine Derivative on the Adhesion between Rubber Compounds and a Brass-Plated Steel Cord. *J. Adhes. Sci. Technol.* **2001**, *15*, 689−701.
(39) Baldwin, F. P.; Buckley, D. J.; Kuntz, I.; Robison, S. B. Preparation and Properties of Chlorobutyl. *Rubber Plast. Age* **1961**, *42*, p 500.
(40) Hendrikse, K. G.; Mcgill, W. J. Vulcanization of Chlorobutyl Rubber. II. A Revised Cationic Mechanism of $ZnO/ZnCl_2$ Initiated Crosslinking. *J. Appl. Polym. Sci.* **2000**, *78*, 2302−2310.

DOI: 10.1021/acsami.5b02887
ACS Appl. Mater. Interfaces 2015, 7, 14317−14327